

# Displacement Dynamics of Fluorine Atoms Reacting with Allyl Bromide Molecules

Z. Z. Zhu, D. J. Smith, and R. Grice\*

Chemistry Department, University of Manchester, Manchester M13 9PL, UK

Received: October 12, 1993; In Final Form: February 8, 1994\*

Reactive scattering of F atoms with  $C_3H_5Br$  molecules leading to Br atom displacement has been studied at an initial translational energy  $E \sim 40 \text{ kJ mol}^{-1}$  using a supersonic beam of F atoms seeded in He buffer gas. The center-of-mass angular distribution of  $C_3H_5F$  scattering shows a broad peak in the forward direction with roughly constant relative intensity  $\sim 0.4$  in the backward hemisphere. The product translational energy distribution peaks at a low fraction  $f'_{pk} \sim 0.1$  of the total available energy with a tail extending up to higher energy. The reaction dynamics involve a stripping mechanism whereby the F atom adds to the  $C=C$  double bond, forming either the secondary fluorobromopropyl radical which dissociates directly to form allyl fluoride reaction product by bonding to the terminal  $CH_2$  group or the primary fluorobromopropyl radical which may dissociate by ring closure to form fluorocyclopropane reaction product by bonding to the intermediate CH group. The suggested occurrence of two reaction pathways is inferred from the absence of H atom or  $CH_2Br$  radical displacement pathways since the mass spectrometer detector does not distinguish between the proposed reaction products.

## Introduction

The reactive scattering arising from Cl atom addition to the  $C=C$  double bond of allyl bromide molecules was among the first systems to be studied<sup>1</sup> in reactive scattering experiments. A "bond migration" mechanism was proposed whereby Br atom displacement followed Cl atom bonding to the terminal  $CH_2$  group of  $C_3H_5Br$ . Reactive scattering of F atoms with vinyl bromide molecules reported in the preceding paper<sup>2</sup> shows a short-lived collision complex mechanism for the formation of  $C_2H_3F$  reaction products. In this case, it was proposed<sup>2</sup> that Br atom displacement arises partly from F atom bonding to the terminal  $CH_2$  group of  $C_2H_3Br$  followed by F atom migration to the  $CHBr$  group as well as from the direct F atom bonding to the  $CHBr$  group. In contrast, F atom addition to allyl iodide molecules<sup>3</sup> shows a stripping mechanism for the formation of  $C_3H_5F$  reaction products. This was attributed<sup>3</sup> in part to "bond migration" following F atom bonding to the terminal  $CH_2$  group of  $C_3H_5I$  and also to the formation of fluorocyclopropane reaction product arising from F atom bonding to the intermediate CH group followed by ring closure displacement of the I atom. However, the I atom displacement reaction of  $F + C_3H_5I$  is significantly more exoergic than the Br atom displacement reaction of  $F + C_2H_3Br$  so that these mechanistic distinctions may be provoked by the energetic differences of the potential energy surfaces. In order to define the mechanistic situation more clearly, reactive scattering measurements have been undertaken on the Br atom displacement reaction of F atoms with  $C_3H_5Br$  molecules which is less exoergic than the Br atom displacement reaction with  $C_2H_3Br$



## Experimental Method

The apparatus was the same as that previously employed in studies of F atom reactive scattering with  $C_2H_3Br$  molecules.<sup>2</sup> The allyl bromide beam issued from a glass nozzle of diameter 0.15 mm with a stagnation pressure  $\sim 100$  mbar maintained by a reservoir at  $30^\circ\text{C}$ . The allyl bromide beam velocity distribution measured by the rotatable mass spectrometer detector peaked at  $\sim 625 \text{ m s}^{-1}$  with a full width  $\sim 270 \text{ m s}^{-1}$  at half-maximum intensity corresponding to a Mach number  $M \sim 4$ .

## Results

Angular distribution measurements of  $C_3H_5F$  reactive scattering yield  $\sim 30 \text{ counts s}^{-1}$  against a background  $\sim 15 \text{ counts s}^{-1}$ .

\* Abstract published in *Advance ACS Abstracts*, March 15, 1994.

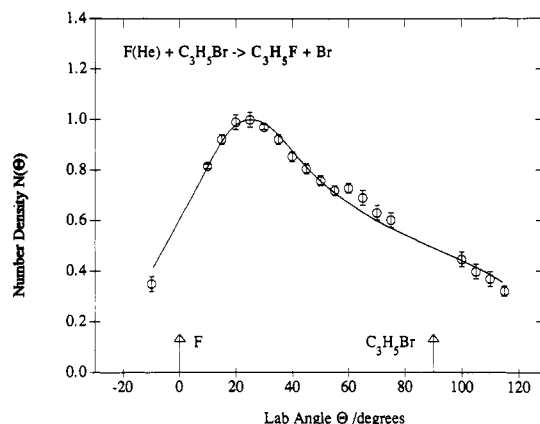


Figure 1. Laboratory angular distribution (number density) of  $C_3H_5F$  reactive scattering from  $F + C_3H_5Br$  at an initial translational energy  $E \sim 40 \text{ kJ mol}^{-1}$ . Solid line shows the fit of the stochastic kinematic analysis.

The laboratory angular distribution of  $C_3H_5F$  number density shown in Figure 1 exhibits a broad peak close to the F atom beam with lower intensity extending out to wide angles. Laboratory velocity distributions of  $C_3H_5F$  flux shown in Figure 2 were measured using integration times  $\sim 6000 \text{ s}$  to gain signal-to-noise ratios  $\sim 10$  at the peaks of the distributions. Kinematic analysis of these data has been performed using the stochastic method<sup>4</sup> with the center-of-mass differential cross section expressed as a product of an angular function  $T(\theta)$  and a velocity function  $U(u, \theta)$ , which is parametrically dependent on scattering angle

$$I_{cm}(\theta, u) = T(\theta) U(u, \theta) \quad (2)$$

The resulting angular function and product translational energy distributions  $P(E')$  are shown in Figure 3 together with the initial translational energy distribution. The angular distribution shows a broad peak in the forward direction which declines to a roughly constant relative intensity  $\sim 0.4$  in the backward hemisphere. The product translational energy distribution peaks at quite low energy with a tail extending out to higher energy. The peak translational energy is slightly higher for scattering in the forward and backward directions than for the sideways scattering. The peak  $E'_{pk}$  and average  $E'_{av}$  product translational energies are listed in Table 1, together with the initial translational energy  $E$

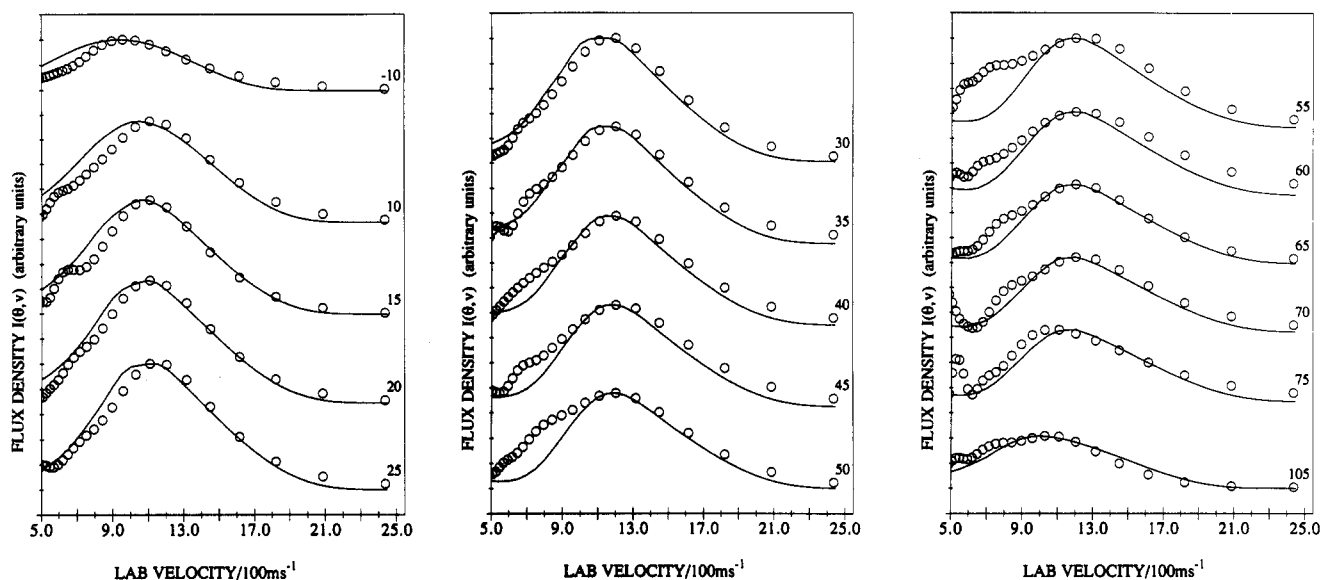
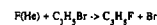
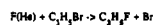


Figure 2. Laboratory velocity distributions (flux density) of reactively scattered C<sub>3</sub>H<sub>5</sub>F from F + C<sub>3</sub>H<sub>5</sub>Br at an initial translational energy  $E \sim 40$  kJ mol<sup>-1</sup>. Solid lines show the fit of the stochastic kinematic analysis.

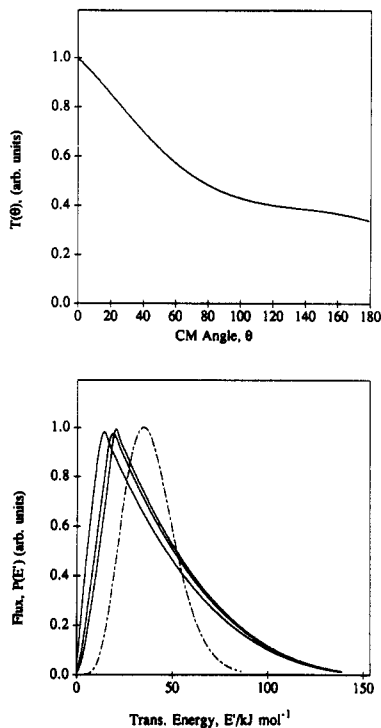
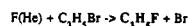


Figure 3. Angular function  $T(\theta)$  and product translational energy distribution  $P(E')$  at an initial translational energy  $E \sim 40$  kJ mol<sup>-1</sup>. Leftmost translational energy distribution corresponds to  $\theta = 90^\circ$  and right most distributions to  $\theta = 0^\circ$  and  $180^\circ$ . Dashed energy curve shows the distribution of initial translational energy.

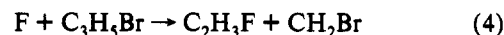
TABLE 1: Reaction Energetics (kJ mol<sup>-1</sup>): Peak Product Translational Energy  $E'_{pk}$ , Average Product Translational Energy  $E'_{av}$ , and Reaction Exoergicity  $\Delta D_0$  at Initial Translational Energy  $E = 40$  kJ mol<sup>-1</sup>

forward-backward		sideways		$\Delta D_0$
$E'_{pk}$	$E'_{av}$	$E'_{pk}$	$E'_{av}$	
20	45	15	40	141

and the reaction exoergicity  $\Delta D_0$  calculated using the bond dissociation energies of C<sub>3</sub>H<sub>5</sub>F from Dahlike and Kass<sup>5</sup> and C<sub>3</sub>H<sub>5</sub>Br from Traeger.<sup>6</sup> No evidence could be detected for reactive scattering from the H atom displacement pathway

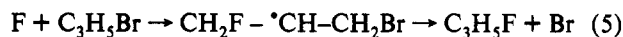


nor for the CH<sub>2</sub>Br radical displacement pathway

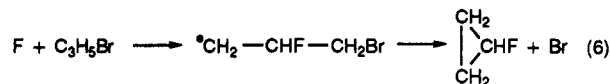


### Discussion

The angular distribution of C<sub>3</sub>H<sub>5</sub>F reactive scattering is characteristic of stripping dynamics in contrast to the short-lived collision complex dynamics of the C<sub>2</sub>H<sub>3</sub>F scattering from the F + C<sub>2</sub>H<sub>3</sub>Br reaction. Reaction is initiated by addition of the F atom to the C=C double bond of C<sub>3</sub>H<sub>5</sub>Br, with a direction of approach which is perpendicular to the plane of the CH<sub>2</sub>=CH moiety. Bonding to the  $\pi$  orbitals is initially symmetrical, but the reaction pathway bifurcates to form a classical fluorobromopropyl radical. If the F atom bonds to the CH<sub>2</sub> group of C<sub>3</sub>H<sub>5</sub>Br, the resulting secondary 1-fluoro-3-bromopropyl radical can dissociate directly by Br atom displacement



However, if the F atom bonds to the intermediate CH group of C<sub>3</sub>H<sub>5</sub>Br, the resulting primary 2-fluoro-3-bromopropyl radical can dissociate by Br atom displacement in the absence of migration, only by ring closure forming the fluorocyclopropane reaction product



These reaction pathways are shown in Figure 4 where the exoergicity of the pathway of eq 6 is estimated relative to that of the pathway of eq 5 by reference to the difference in the heats of formation of cyclopropane and propene.<sup>7</sup> *Ab initio* calculations<sup>8</sup> of F atom addition to C<sub>2</sub>H<sub>4</sub> molecules show that the bond dissociation energy of the fluoroethyl radical  $D_0(F-C_2H_4) = 165$  kJ mol<sup>-1</sup> exceeds the exoergicity of the reaction pathway of eq 5 by only  $\sim 24$  kJ mol<sup>-1</sup>. The secondary radical intermediate of eq 5 is more stable<sup>9</sup> by  $\sim 14$  kJ mol<sup>-1</sup> than the primary radical intermediate of eq 6. Hence, the stability  $\sim 43$  kJ mol<sup>-1</sup> of the primary radical intermediate of eq 6 with respect to reaction products represents a more significant fraction of the reaction exoergicity  $\sim 108$  kJ mol<sup>-1</sup> than is the case for the secondary

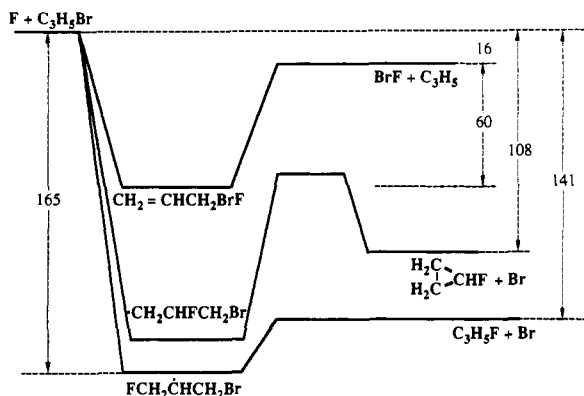
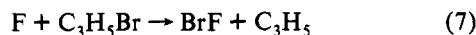


**Figure 4.** Potential energy profiles for the reaction pathways of  $F + C_3H_5Br$  leading to Br atom abstraction and Br atom displacement, showing free radical intermediates.

**TABLE 2: Potential Energy Barriers (kJ mol<sup>-1</sup>) Estimated for Decomposition of the Primary  $\cdot CH_2CHFCH_2Br$  Radical Intermediate,  $E_b$  for Radical Decomposition and  $E_a$  for Radical Reassociation, and  $\Delta D_0$  Reaction Exoergicity**

pathway	$E_b$	$E_a$	$\Delta D_0$
eq 3	120	20	53
eq 4	90	30	92
eq 6	80	35	108

radical intermediate of eq 5. The potential energy barrier  $E_a \sim 70$  kJ mol<sup>-1</sup> for the ring opening reaction of I atoms with cyclopropane molecules<sup>10</sup> corresponds to a potential energy barrier  $E_b \sim 80$  kJ mol<sup>-1</sup> to the reverse ring closure. The same potential energy barrier is employed here for the ring closure of eq 6 as shown in Figure 4. The potential energy barrier to F atom migration  $E_b \sim 120$  kJ mol<sup>-1</sup> in the F atom bridging configuration<sup>8</sup> is much higher than the potential energy barrier  $E_b \sim 80$  kJ mol<sup>-1</sup> required for Br atom displacement via ring closure. The potential energy barrier for ring closure is also less than that required for H atom displacement  $E_b \sim 127$  kJ mol<sup>-1</sup> or for  $CH_2Br$  radical displacement  $E_b \sim 98$  kJ mol<sup>-1</sup>, making ring closure the lowest-energy pathway for dissociation of the primary  $\cdot CH_2CHFCH_2Br$  radical, as shown in Table 2. The F atom reactive scattering measurements with  $C_2H_3Br$  molecules<sup>2</sup> indicate that F atom migration competes with H atom displacement with the barrier to F atom migration exceeding that of H atom displacement. Consequently, the absence of reaction products from the H atom displacement pathway of eq 3 suggests that decomposition of the primary 2-fluoro-3-bromopropyl radical intermediate follows the ring closure pathway of eq 6. Both the allyl fluoride product of eq 5 and the fluorocyclopropane product of eq 6 will form  $C_3H_5F^+$  ions in the ion source of the mass spectrometer detector so that the contributions of these reaction products to the angular and velocity distributions of Figures 2 and 3 are not separately identified. The Br atom abstraction pathway



has been observed<sup>11</sup> to follow a long-lived complex mechanism in a manner similar to the I atom abstraction pathway of the  $F + C_3H_5I$  reaction.<sup>12,13</sup> The Br atom abstraction pathway involves a stable allyl bromofluoride radical intermediate as shown in Figure 4.

The product translational energy distribution for sideways scattering is compared in Figure 5 with the prediction of phase space theory<sup>14</sup> calculated using the full 21 vibrational modes of allyl fluoride<sup>15</sup> reaction product with maximum initial  $b_m = 3.6$  Å and final  $b'_m = 3.0$  Å impact parameters. The experimental distribution extends out to higher translational energy than the phase space prediction, indicating that energy is incompletely

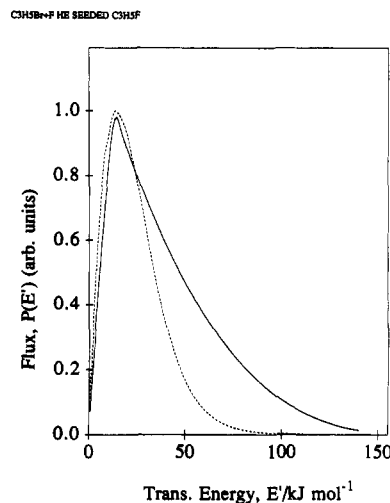


**Figure 5.** Product translational energy distribution for  $F + C_3H_5Br$  sideways scattering at initial translational energy  $E \sim 40$  kJ mol<sup>-1</sup> shown by a solid curve compared with the phase space prediction shown by a broken curve.

randomized over the internal modes of the  $C_3H_5F$  reaction products. Indeed, the microcanonical prior distribution<sup>16</sup> for the fraction  $f' = E'/(E + \Delta D_0)$  of total available energy disposed into product translation

$$P(f') \propto f'^{1/2}(1-f')^n \quad (8)$$

gives good agreement with the experimental distribution when the parameter  $n = 5-6$  is employed. A rotational period  $\tau_{rot} \sim 3.0$  ps may be estimated for an  $FCH_2-\cdot CH-CH_2Br$  radical intermediate formed in collisions with the maximum initial orbital angular momentum  $L_m \sim 200\hbar$ . In contrast to the angular distribution for the  $F + C_2H_3Br$  reactive scattering,<sup>2</sup> there is no evidence for a backward peak corresponding to the forward peak in the  $F + C_3H_5Br$  angular distribution of Figure 3. This indicates that the lifetime  $\tau < 1.5$  ps of the secondary radical intermediate must be less than half its rotational period in the reaction pathway of eq 4. A longer lifetime would be anticipated for the primary radical intermediate in the reaction pathway of eq 6 which dissociates via ring closure. Indeed, a less strongly forward peaked distribution may contribute to the angular and product translational energy distributions of Figure 3 without being separately identified, particularly if addition to the terminal  $CH_2$  group were the favored reaction pathway. These results for the  $F + C_3H_5Br$  reaction remain very similar to those for the  $F + C_3H_5I$  reaction<sup>3</sup> since the stability of the primary radical of eq 6 is very similar in each case while the secondary radical of eq 5 has a minimal stability and a short collision lifetime. Indeed, Br atom displacement in the  $F + C_3H_5Br$  reaction is now less exoergic than is the case for the  $F + C_2H_3Br$  reaction. The estimated lifetime of the  $FCH_2-\cdot CH-CH_2Br$  intermediate in the  $F + C_3H_5-Br$  reaction is less than that of the  $\cdot CH_2-CHBrF$  intermediate in the  $F + C_2H_3Br$  reaction. This is in accord with the role of F atom migration in the  $FCH_2-\cdot CH-CH_2Br$  radical which prolongs the lifetime over that of the more complex  $FCH_2-\cdot CH-CH_2Br$  radical where rearrangement of the bonding leads directly to Br atom displacement.

In the case of the  $Cl + C_3H_5Br$  reaction,<sup>1</sup> the barrier to Cl atom migration<sup>17</sup> in the  $\cdot CH_2-CHCl-CH_2Br$  radical formed by Cl atom addition to the intermediate CH group,  $E_b \sim 26$  kJ mol<sup>-1</sup>, is lower than the barrier to Br atom displacement via ring closure. Consequently,  $C_3H_5Cl$  reaction products are expected to be formed in the  $Cl + C_3H_5Br$  reaction entirely by Br atom displacement from the  $ClCH_2-\cdot CH-CH_2Br$  radical. Thus, the conclusion<sup>1</sup> that Br atom displacement from  $C_2H_3Br$  and  $C_3H_5-Br$  occurs exclusively by anti-Markovnikov addition to the terminal

CH<sub>2</sub> group of both molecules may apply in the case of the Cl atom reactions due to the low barrier to Cl atom migration, but a diversity of reaction pathways applies to the F atom reactions<sup>2</sup> due to the much higher barrier to F atom migration.

**Acknowledgment.** Support of this work by SERC and the European Commission is gratefully acknowledged.

#### References and Notes

- (1) Cheung, J. T.; McDonald, J. D.; Herschbach, D. R. *J. Am. Chem. Soc.* **1973**, *95*, 7889.
- (2) Zhu, Z. Z.; Smith, D. J.; Grice, R. *J. Phys. Chem.*, preceding paper in this issue.
- (3) Zhu, Z. Z.; Smith, D. J.; Grice, R. *Int. J. Mass Spectrom. Ion Processes*, in press.

- (4) Entemann, E. A.; Herschbach, D. R. *Discuss. Faraday Soc.* **1967**, *44*, 289.
- (5) Dahlke, G. D.; Kass, S. R. *J. Am. Chem. Soc.* **1991**, *113*, 5566.
- (6) Traeger, J. C. *Int. J. Mass Spectrom. Ion Processes* **1984**, *58*, 259.
- (7) Pedley, J. B.; Naylor, R. D.; Kirby, S. P. *Thermochemical Data of Organic Compounds*, 2nd ed.; Chapman and Hall: London, 1986.
- (8) Engels, B.; Peyerimhoff, S. D. *J. Phys. Chem.* **1989**, *93*, 4462.
- (9) Benson, S. W. *Thermochemical Kinetics*; Wiley: New York, 1968.
- (10) Ogg, R. A.; Priest, W. J. *J. Chem. Phys.* **1939**, *7*, 736.
- (11) Zhu, Z. Z.; Smith, D. J.; Grice, R. To be published.
- (12) Harkin, J. J.; Smith, D. J.; Grice, R. *Mol. Phys.* **1991**, *72*, 763.
- (13) White, R. W. P.; Smith, D. J.; Grice, R. *J. Phys. Chem.* **1993**, *97*, 2123.
- (14) Light, J. C. *Discuss. Faraday Soc.* **1967**, *44*, 14.
- (15) Durig, J. R.; Zhen, M.; Hensel, H. L.; Joseph, P. J.; Groner, P.; Little, T. S. *J. Phys. Chem.* **1985**, *89*, 2877.
- (16) Bernstein, R. B.; Levine, R. D. *Adv. At. Mol. Phys.* **1975**, *11*, 215.
- (17) Engels, B.; Peyerimhoff, S. D.; Skell, D. S. *J. Phys. Chem.* **1990**, *94*, 1267.